Compressible Laminar Boundary Layers with Suction on Swept and Tapered Wings

Kalle Kaups* and Tuncer Cebeci†
Douglas Aircraft Company, Long Beach, Calif.

In this paper we present a numerical method for solving the compressible laminar boundary-layer equations with suction on swept and tapered wings. The method employs an efficient two-point finite-difference method to solve the governing equations, and a very convenient similarity transformation which removes the wall normal velocity as a boundary condition and places it into the governing equations as a parameter. In this way the awkward nonlinear boundary condition which couples all the variables is avoided. To test and demonstrate the method, we present a sample calculation for a typical laminar-flow-control (LFC) wing.

Nomenclature

c = ρ_e/ρ or local streamwise chord length
c_{f_x} = local skin-friction coefficient based on components in the negative x-coordinate direction
c_{f_θ} = local skin-friction coefficient based on components in θ-coordinate direction
C = dimensionless density-viscosity parameter, $\rho\mu/(\rho\mu)_e$
C_p = pressure coefficient $2(p_e - p_\infty)/(\rho_\infty U_\infty^2)$
E = total enthalpy ratio, H/H_e
f,g = transformed vector potential for x,ϕ, respectively
f',g' = as defined in Eq. (25)
H = total enthalpy
K = variable grid factor
m_1 to m_5 = dimensionless pressure-gradient parameters
M_∞ = freestream Mach number
p = static pressure
Pr = Prandtl number
R_x = $u_e x/\nu_e$, Reynolds number based on x
$R_{\delta^*_x}$ = $u_e\delta^*_x/\nu_e$, Reynolds number based on displacement thickness
$R_{\delta^*_\theta}$ = $w_e\delta^*_\theta/\nu_e$, Reynolds number based on displacement thickness
s = arc length along θ-coordinate line for $x=x_0$ measured from the stagnation line
T = static temperature
u = velocity component in x-coordinate direction
u_s = resultant velocity at the edge of boundary layer
$\bar{u}$ = $-u$
U_∞ = freestream velocity
v = velocity component normal to the surface, y-coordinate direction
w = velocity component in θ-coordinate direction
w_θ = $dw/d\theta$
x,θ,y = polar coordinate system in the developed plane of the wing surface
$\bar{x},\bar{y},\bar{z}$ = Cartesian coordinate system used for wing definition: $\bar{x}$ is chordwise, and $\bar{y}$ is spanwise; $\bar{z}=0$ is the wing chord plane.
δ = boundary-layer thickness
δ^*_x = displacement thickness based on the velocity components in the negative x-coordinate direction
δ^*_θ = displacement thickness based on the velocity components in the θ-coordinate direction
η = similarity variable
θ = polar coordinate in the developed plane or momentum thickness
θ_x = momentum thickness based on velocity components in the negative x-direction
θ_θ = momentum thickness based on the velocity components in the θ-direction
λ_1 = sweep angle of the leading edge
λ_2 = sweep angle of the trailing edge
μ = dynamic viscosity
ν = kinematic viscosity
ξ/c = fraction of streamwise wing chord
ρ = density
ϕ = stretching variable, $\xi/c = 1-\cos\phi$
Φ,ψ = two-component vector potential

Subscripts

e = edge of boundary layer
0 = defining airfoil section
w = wall
∞ = freestream conditions

primes denote differentiation with respect to η

Introduction

In preliminary design for the purpose of rapid estimation of performance of three-dimensional configurations, it is often convenient to use simplified two-dimensional or semi-three-dimensional flow calculations to avoid lengthy and expensive calculations. Sometimes the design requirement is such that the simplified flow calculations are quite accurate for most of the configuration. For example, let us consider the laminar-flow-control (LFC) wing for a long-range transport. From the standpoint of the suction system optimization, it is desirable and necessary to keep the spanwise pressure gradient to a minimum on such a wing. Ideally, this situation corresponds to pressure isobars along constant percent-chord lines or along the generators if the wing has trapezoidal planform. Straight isobars are very difficult to obtain near the wingroot or wingtip; for this reason these regions are excluded from consideration. Limiting our attention to wings with trapezoidal planform, we can deduce that the absence of pressure gradient along the generators is equivalent to the conical-flow assumption. In order to obtain a truly conical surface, we can ignore the wing twist and represent the thickness distribution by geometrically similar sections. The conical-flow assumption enables the governing

Received Oct. 6, 1976; revision received April 1, 1977.
Index categories: Aerodynamics; Boundary Layers and Convective Heat Transfer – Laminar.
*Senior Engineer/Scientist. Member AIAA.
†Chief Aerodynamics Engineer – Research. Member AIAA.

three-dimensional flow equations to be written in a form similar to two-dimensional flow equations by using similarity transformations. In case of flows with mass transfer, similarity imposes restrictions on the distribution of spanwise wall mass flow rate. Even then, however, the restrictions are not that severe and similarity ideas can still be used for such cases with reasonable accuracy.

In this paper we present an efficient finite-difference numerical method for solving the compressible laminar boundary-layer equations with suction on swept and tapered wings. The method, which employs a very convenient transformation, is described in the following sections.

Boundary-Layer Equations

The governing boundary-layer equations for a three-dimensional compressible laminar flow in a polar coordinate system embedded in the surface (see Fig. 1) under the conical-flow approximation ($\partial p/\partial x \equiv 0$) are given by the following equations:

Continuity equation

$$\frac{\partial}{\partial x}(\rho x u) + \frac{\partial}{\partial \theta}(\rho w) + \frac{\partial}{\partial y}(\rho x v) = 0 \tag{1}$$

x-momentum equation

$$\rho u \frac{\partial u}{\partial x} + \rho \frac{w}{x}\frac{\partial u}{\partial \theta} + \rho v \frac{\partial u}{\partial y} - \rho \frac{w^2}{x} = \frac{\partial}{\partial y}\left(\mu \frac{\partial u}{\partial y}\right) \tag{2}$$

θ-momentum equation

$$\rho u \frac{\partial w}{\partial x} + \rho \frac{w}{x}\frac{\partial w}{\partial \theta} + \rho v \frac{\partial w}{\partial y} + \rho \frac{uw}{x} = -\frac{1}{x}\frac{dp}{d\theta} + \frac{\partial}{\partial y}\left(\mu \frac{\partial w}{\partial y}\right) \tag{3}$$

Energy equation

$$\rho u \frac{\partial H}{\partial x} + \rho \frac{w}{x}\frac{\partial H}{\partial \theta} + \rho v \frac{\partial H}{\partial y} = \frac{\partial}{\partial y}\left[\frac{\mu}{Pr}\frac{\partial H}{\partial y} + \mu\left(1 - \frac{1}{Pr}\right)\frac{\partial}{\partial y}\left(\frac{u^2 + w^2}{2}\right)\right] \tag{4}$$

Here x is the distance along the generator from the origin 0, θ is the polar angle in the developed plane measured from the stagnation line, and y is the distance normal to the surface. The corresponding velocity components are u, w, and v, respectively; and $\bar{x}$, $\bar{y}$, $\bar{z}$ denote the Cartesian coordinate system in which the wing is defined.

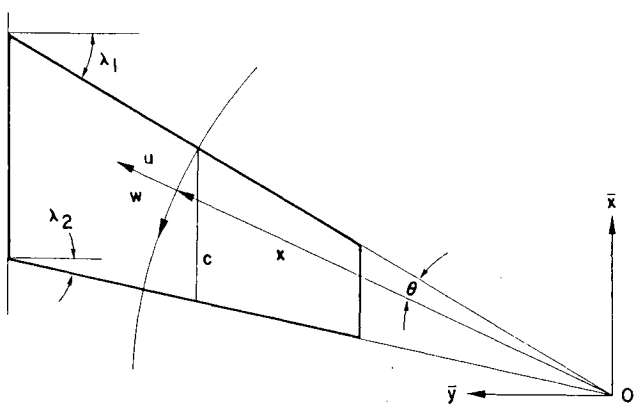

Fig. 1 Tapered wing and the polar coordinate system.

The boundary conditions for the velocity and temperature fields are

$$y = 0 \quad u = 0 \quad v = v_w \quad w = 0 \quad (\partial H/\partial y)_w = 0 \tag{5a}$$

$$y \to \delta \quad u \to u_e \quad H \to H_e \quad w \to w_e \tag{5b}$$

Along the stagnation line Eq. (3) is singular because $w = 0$. Differentiating it with respect to θ and setting $w = 0$, we obtain the following equations for the stagnation line:

Continuity equation

$$\frac{\partial}{\partial x}(\rho u x) + \rho w_\theta + \frac{\partial}{\partial y}(\rho v x) = 0 \tag{6}$$

x-momentum equation

$$\rho u \frac{\partial u}{\partial x} + \rho v \frac{\partial u}{\partial y} = \frac{\partial}{\partial y}\left(\mu \frac{\partial u}{\partial y}\right) \tag{7}$$

θ-momentum equation

$$\rho u \frac{\partial w_\theta}{\partial x} + \rho \frac{w_\theta^2}{x} + \rho v \frac{\partial w_\theta}{\partial y} + \rho u \frac{w_\theta}{x} = \frac{1}{x}\frac{\partial^2 p_\theta}{\partial \theta^2} + \frac{\partial}{\partial y}\left(\mu \frac{\partial w_\theta}{\partial y}\right) \tag{8}$$

Energy equation

$$\rho u \frac{\partial H}{\partial x} + \rho v \frac{\partial H}{\partial y} = \frac{\partial}{\partial y}\left[\frac{\mu}{Pr}\frac{\partial H}{\partial y} + \mu\left(1 - \frac{1}{Pr}\right)\frac{\partial}{\partial y}\left(\frac{u^2}{2}\right)\right] \tag{9}$$

The boundary conditions of Eqs. (6-9) are the same as those given by Eq. (5), except now the outer boundary condition imposed on w is replaced by

$$\text{as } y \to \delta \qquad w_\theta \to w_{\theta e} \tag{10}$$

In the present calculations we treat air as a perfect gas and use the Sutherland's viscosity law for μ. The Prandtl number is assumed constant.

Geometry and External Velocity Distribution

Since boundary-layer calculations are done along the arc formed by the intersection of a sphere of radius $x = x_0$ and the conical wing surface, the independent variable θ must be calculated from the geometrical data. We assume that the

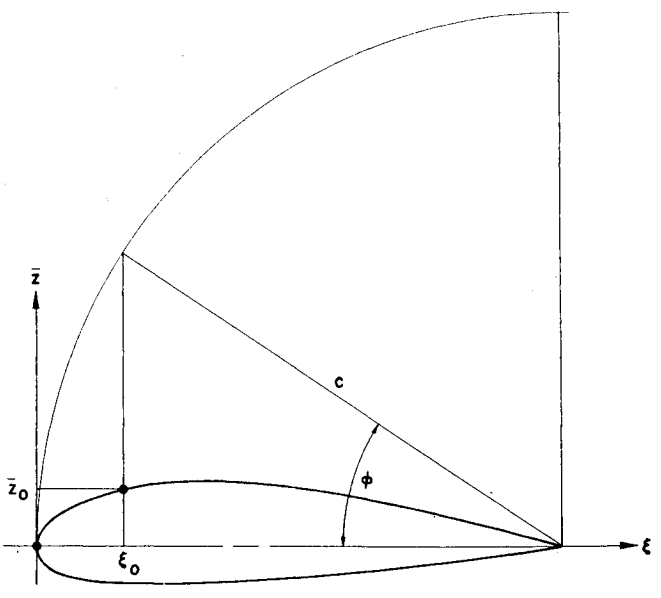

Fig. 2 Variables related to the input streamwise airfoil definition.

wing planform is given in terms of the sweep angles λ_1 and λ_2 for the leading and trailing edges, respectively. In addition, we assume that the nondimensional wing-thickness distribution $\bar{z}/c$ is specified along a streamwise section with chord length c. This chord intersects the sphere at the wing leading edge as shown in Fig. 1. To avoid double-valued functions in wing definitions we express ξ/c in terms of a new variable ϕ defined by (see Fig. 2)

$$\xi/c = 1 - \cos\phi \tag{11}$$

Here the negative values of $\bar{z}/c$ imply negative ϕ, and $\phi = 0$ designates the leading edge. The variable θ is obtained from the integration of the following expressions which relate the Cartesian coordinate system to the polar coordinate system,

$$\frac{d\theta}{d\phi} = \frac{1}{x_0}\sqrt{\left(\frac{d\bar{x}}{d\phi}\right)^2 + \left(\frac{d\bar{y}}{d\phi}\right)^2 + \left(\frac{d\bar{z}}{d\phi}\right)^2} \tag{12}$$

where

$$x_0 = \frac{c}{\cos\lambda_1[\tan\lambda_1 - \tan\lambda_2]} \tag{13}$$

$$\frac{d\bar{x}}{d\phi} = \frac{1}{\cos\lambda_1 h^{1/2}}\left\{c\sin\phi + \frac{[x_0\sin\lambda_1 - c(1-\cos\phi)]}{2h}\frac{dh}{d\phi}\right\} \tag{14}$$

$$\frac{d\bar{y}}{d\phi} = \frac{x_0}{2h^{3/2}}\frac{dh}{d\phi} \tag{15}$$

$$\frac{d\bar{z}}{d\phi} = \frac{c}{\cos\lambda_1 h^{1/2}}\left[\frac{d(\bar{z}/c)_0}{d\phi} - \frac{(\bar{z}/c)_0}{2h}\frac{dh}{d\phi}\right] \tag{16}$$

$$h = 1 + \frac{c^2}{(x_0\cos\lambda_1)^2}\left(\frac{\bar{z}}{c}\right)_0^2 + \left[\tan\lambda_1 - \frac{c(1-\cos\phi)}{x_0\cos\lambda_1}\right]^2 \tag{17}$$

Here $(\bar{z}/c)_0$ denotes the ordinate of the defining airfoil. It is obtained by spline-fitting the data $\bar{z}$ vs ϕ. Integration of Eq. (12) starts from the stagnation line where $\theta = 0$.

To calculate the inviscid velocity components $\bar{u}_e$ and w_e from the input pressure coefficient C_p, we use the expression

$$\frac{d\bar{u}_e}{d\theta} = -w_e = -\sqrt{u_s^2 - \bar{u}_e^2} \tag{18}$$

which follows from the conical-flow relationships expressed in surface polor coordinates. Here u_s is the resultant inviscid velocity obtained from the input C_p values. Equation (18) is a nonlinear differential equation for $\bar{u}_e$. It is integrated by the fourth-order Runge-Kutta method with the initial condition $u_s = \bar{u}_e$ at $\theta = 0$.

Similarity Transformation for Laminar Flows

In accordance with similarity conditions for conical flow, we define

$$d\eta = \sqrt{\frac{\bar{u}_e}{\rho_e\mu_e x}}\rho dy \tag{19}$$

and introduce a two-component vector potential satisfying the continuity equation (1),

$$\rho\bar{u}x = \frac{\partial\psi}{\partial y} \quad \rho wx = \frac{\partial\Phi}{\partial y} \quad \rho vx = \frac{\partial\psi}{\partial x} - \frac{1}{x}\frac{\partial\Phi}{\partial\theta} + (\rho vx)_w \tag{20}$$

together with dimensionless parameters f and g for ψ and Φ,

$$\psi = x^{3/2}\sqrt{\rho_e\mu_e\bar{u}_e}\, f(\eta,\theta) \tag{21a}$$

$$\Phi = x^{3/2}\sqrt{\rho_e\mu_e\bar{u}_e}\, w_e/\bar{u}_e\, g(\eta,\theta) \tag{21b}$$

where $\bar{u} = -u$ and $\bar{u}_e = -u_e$. With the relations given by Eqs. (19-21), Eqs. (1-4) can be written as

$$(Cf'')' + m_1 f''f + m_2 gf'' - m_3^2[(g')^2 - f'g'] + m_4 f'' = m_3\left(g'\frac{\partial f'}{\partial\theta} - f''\frac{\partial g}{\partial\theta}\right) \tag{22}$$

$$(Cg'')' + m_1 g''f + m_2 gg'' + + m_5[c - (g')^2] - [c - f'g'] + m_4 g'' = m_3\left(g'\frac{\partial g'}{\partial\theta} - g''\frac{\partial g}{\partial\theta}\right) \tag{23}$$

$$\left[\frac{CE'}{Pr} + \frac{C\bar{u}_e^2}{H_e}\left(1 - \frac{1}{Pr}\right)(f'f'' + m_3^2 g'g'')\right]' + m_1 E'f + m_2 E'g + m_4 E' = m_3\left(g'\frac{\partial E}{\partial\theta} - E'\frac{\partial g}{\partial\theta}\right) \tag{24}$$

Here

$$f' = \bar{u}/\bar{u}_e \quad g' = w/w_e \quad E = H/H_e \quad C = \rho\mu/\rho_e\mu_e \quad c = \rho_e/\rho \tag{25a}$$

$$m_1 = -1.5 \quad m_2 = m_5 + 0.5m_3^2 + \frac{0.5m_3}{(\rho\mu)_e}\frac{d(\rho\mu)_e}{d\theta} \quad m_3 = \frac{w_e}{\bar{u}_e} \tag{25b}$$

$$m_4 \frac{-(\rho v)_w}{(\rho\bar{u})_e}(R_x)^{1/2} \qquad m_5 = \frac{1}{\bar{u}_e}\frac{dw_e}{d\theta} \qquad R_x = \frac{\bar{u}_e x}{\nu_e} \tag{25c}$$

The boundary conditions given by Eq. (5) become

$$\eta = 0 \qquad f = g = f' = g' = 0 \qquad E'_w = 0 \tag{26a}$$

$$\eta = \eta_\infty \qquad f' = g' = E = 1 \tag{26b}$$

The stagnation-line equations (6-9) can be transformed and expressed in a form similar to those given by Eqs. (22-24). Because of the singularity in w, we make the following changes in Eqs. (20) and (21)

$$\rho w_\theta = \partial\Phi/\partial y \qquad \rho xv = (\partial\psi/\partial x) - \Phi + (\rho xv)_w \tag{27}$$

$$\Phi = \sqrt{\rho_e\mu_e\bar{u}_e x}\frac{w_{\theta e}}{\bar{u}_e}g(\eta) \tag{28}$$

Application of the modified transformation to Eqs. (7-9) yields

$$[Cf'']' + m_1 f''f + m_5 gf'' + m_4 f'' = 0 \tag{29}$$

$$[Cg'']' + m_1 g''g + m_5[c - (g')^2] - [c - f'g'] + m_4 g'' = 0 \tag{30}$$

$$\left[\frac{CE'}{Pr} + \frac{C\bar{u}_e^2}{H_e}\left(1 - \frac{1}{Pr}\right)ff''\right]' + m_1 E'f + m_5 E'g + m_4 E' = 0 \tag{31}$$

The definitions of various terms in Eqs. (29-31) are the same as those defined in Eq. (25) except that

$$g' = w_\theta / w_{\theta e} \tag{32}$$

The boundary conditions for Eqs. (21-23) are given by Eq. (26).

For similarity, the coefficients m_2 to m_5 must be constants, or, at most, functions of θ only. Consequently, the wall mass transfer rate can vary arbitrarily with θ but must vary as $x^{-1/2}$ with x.

Numerical Method

We use Keller's box method[1] to solve the governing equations described in the previous section. This method, extensively used by Cebeci and his associates, is an accurate and efficient method well-suited to solve parabolic partial differential equations. Its application to two-dimensional and three-dimensional flow problems is described in some detail in several references, (see, for example, Refs. 1-4). For this reason, only a brief description of it is presented here.

According to the box method, we write the governing system of partial differential equations in the form of a first-order system. Thus, the derivatives of the dependent variables are introduced as new unknown functions. With the resulting first-order system for a rectangular net defined by

$$\theta_0 = 0 \quad \theta_n = \theta_{n-1} + k_n \quad (n = 1,2,\ldots,N) \tag{33a}$$

$$\eta_0 = 0 \quad \eta_j = \eta_{j-1} + h_j \quad (j = 1,2,\ldots,J;\ \eta_j = \eta_\infty) \tag{33b}$$

we use simple centered-difference quotients and averages at the midpoints of net rectangulars or net segments, as required, to get $O(h^2)$ accurate finite-difference equations. The resulting nonlinear equations are solved by using Newton's method. In order to do this with an efficient computational scheme, a block elimination method discussed in Refs. 2 and 5 is used. It should be noted that in the overall iteration scheme, the two momentum equations are solved independently of the energy equation.

Formulation of the Momentum Equations

We introduce new dependent variables $u(\theta,\eta)$, $v(\theta,\eta)$, $w(\theta,\eta)$, $t(\theta,\eta)$ so that Eqs. (22) and (23) can be written as a first-order system

$$f' = u \tag{34a}$$

$$u' = v \tag{34b}$$

$$g' = w \tag{34c}$$

$$w' = t \tag{34d}$$

$$(Cv)' + m_1 fv + m_2 gv - m_3^2 (w^2 - uw) + m_4 v = m_3 \left(w \frac{\partial u}{\partial \theta} - u \frac{\partial g}{\partial \theta} \right) \tag{34e}$$

$$(Ct)' + m_1 ft + m_2 gt + m_5 (c - w^2) - (c - uw) + m_4 t = m_3 \left(w \frac{\partial w}{\partial \theta} - t \frac{\partial g}{\partial \theta} \right) \tag{34f}$$

The quantities (f, u, v, g, w, t) at points (θ_n, η_j) of the net are approximated by net functions denoted by (f_j^n, u_j^n, v_j^n). The difference equations for Eqs. (34a-34d) are

$$h_j^{-1} (f_j^n - f_{j-1}^n) = u_{j-1/2}^n \tag{35a}$$

$$h_j^{-1} (u_j^n - u_{j-1}^n) = v_{j-1/2}^n \tag{35b}$$

$$h_j^{-1} (g_j^n - g_{j-1}^n) = w_{j-1/2}^n \tag{35c}$$

$$h_j^{-1} (w_j^n - w_{j-1}^n) = t_{j-1/2}^n \tag{35d}$$

Similarly, Eqs. (34e) and (34f) are approximated by centering them on the midpoint $(\theta_{n-1/2}, \eta_{j-1/2})$ of the net rectangle,

$$\begin{aligned} &h_j^{-1} [(Cv)_j^n - (Cv)_{j-1}^n] + m_1^n (fv)_{j-1/2}^n \\ &+ (m_2^n + \alpha_n)(gv)_{j-1/2}^n + [(m_3^2)_{-\alpha_n}](uw)_{j-1/2}^n \\ &- (m_3^2)^n (w^2)_{j-1/2}^n + (m_4^n - \alpha_n g_{j-1/2}^{n-1}) v_{j-1/2}^n \\ &- \alpha_n [w_{j-1/2}^{n-1} u_{j-1/2}^n - u_{j-1/2}^{n-1} w_{j-1/2}^n - v_{j-1/2}^{n-1} g_{j-1/2}^n] = T_{j-1/2}^{n-1} \end{aligned} \tag{35e}$$

$$\begin{aligned} &h_j^{-1} [(Ct)_j^n - (Ct)_{j-1}^n] + m_1^n (ft)_{j-1/2}^n + (m_2^n + \alpha_n)(gt)_{j-1/2}^n \\ &- (m_5^n + \alpha_n)(w^2)_{j-1/2}^n + (uw)_{j-1/2}^n + (m_4^n - \alpha_n g_{j-1/2}^{n-1}) t_{j-1/2}^n \\ &+ \alpha_n t_{j-1/2}^{n-1} g_{j-1/2}^n = S_{j-1/2}^{n-1} \end{aligned} \tag{35f}$$

where

$$T_{j-1/2}^{n-1} = -(L_1)_{j-1/2}^{N-1} + \alpha_n [(vg)_{j-1/2}^{n-1} - (uw)_{j-1/2}^{n-1}] \tag{36a}$$

$$\begin{aligned} (L_1)_{j-1/2}^{n-1} &= h_j^{-1} [(Cv)_j^{n-1} - (Cv)_{j-1}^{n-1}] \\ &+ m_1^{n-1} (fv)_{j-1/2}^{n-1} + m_2^{n-1} (gv)_{j-1/2}^{n-1} \\ &- (m_3^2)^{n-1} [(w^2)_{j-1/2}^{n-1} - (uw)_{j-1/2}^{n-1}] + m_4^{n-1} v_{j-1/2}^{n-1} \\ S_{j-1/2}^{n-1} &= -(L_2)_{j-1/2}^{n-1} + c_{j-1/2}^n [1 - m_5^n] \\ &+ \alpha_n [(tg)_{j-1/2}^{n-1} - (w^2)_{j-1/2}^{n-1}] \\ (L_2)_{j-1/2}^{n-1} &= h_j^{-1} [(Ct)_j^{n-1} - (Ct)_{j-1}^{n-1}] \\ &+ m_1^{n-1} (ft)_{j-1/2}^{n-1} + m_2^{n-1} (gt)_{j-1/2}^{n-1} \\ &+ m_5^{n-1} [c_{j-1/2}^{n-1} - (w^2)_{j-1/2}^{n-1}] - c_{j-1/2}^{n-1} \\ &+ (uw)_{j-1/2}^{n-1} + m_4^{n-1} t_{j-1/2}^{n-1} \end{aligned} \tag{36b}$$

$$\alpha_n = \frac{m_3^{n-1/2}}{\theta_n - \theta_{n-1}}$$

Equations (35) and (36) are imposed for $j = 1$ to $J-1$. For $j = 0$ and $j = j$, we use the boundary conditions given in Eq. (26) to get

$$f_0^n = 0 \quad g_0^n = 0 \quad u_0^n = 0 \quad w_0^n = 0 \quad w_j^n = 1 \quad u_j^n = 1 \tag{37}$$

If we assume $(f_j^{n-1}, u_j^{n-1}, v_j^{n-1}, g_j^{n-1}, w_j^{n-1}, t_j^{n-1})$ to be known for $0 \le j \le J$, then the system given by Eqs. (35-37) yields an implicit nonlinear algebraic system of $6J+6$ equations in as many unknowns, $(f_j^n, u_j^n, v_j^n, g_j^n, w_j^n, t_j^n)$. The system can be solved very effectively by using Newton's method. The details are presented in several references (see, for example, Refs. 1 and 2). The important observations are that the linearized equations obtained by applying Newton's method form a block tridiagonal system (with 6×6 blocks) and that system can be solved very efficiently by the procedure discussed in the aforementioned references.

The solution procedure for the stagnation-line equations is very similar to that discussed earlier. Again, by using the

definitions (34a-34d), we can write Eqs. (29) and (30) as

$$(Cv)' + m_1 fv + m_5 gv + m_4 v = 0 \tag{38a}$$

$$(Ct)' + m_1 gt + m_5 (c - w^2) - c + uw + m_4 t = 0 \tag{38b}$$

The difference equations for Eq. (38) are

$$h_j^{-1}[(Cv)_j^n - (Cv)_{j-1}^n] + m_j^n (fv)_{j-1/2}^n + m_5^n (gv)_{j-1/2}^n + m_4^n v_{j-1/2}^n = 0 \tag{39a}$$

$$h_j^{-1}[(Ct)_j^n - (Ct)_{j-1}^n] + m_1^n (gt)_{j-1/2}^n + m_5^n [c_{j-1/2}^n - (w^2)_{j-1/2}^n] - c_{j-1/2}^n + (uw)_{j-1/2}^n + m_4^n t_{j-1/2}^n = 0 \tag{39b}$$

The boundary conditions for Eqs. (38) and (39) are the same as those given in Eq. (37).

Formulation of the Energy Equation

If we let

$$E' = G \tag{40a}$$

and use the definitions for f', f'', g', g'', then Eq. (24) can be written as

$$\left(\frac{C}{Pr} G\right)' + (b_1)' + b_2 G = m_3 \left(w \frac{\partial E}{\partial \theta} - G \frac{\partial g}{\partial \theta}\right) \tag{40b}$$

Here

$$b_1 = \frac{C\tilde{u}_e^2}{H_e}\left(1 - \frac{1}{Pr}\right)(uv + m_3^2 wt) \tag{41a}$$

$$b_2 = m_1 f + m_2 g + m_4 \tag{41b}$$

The difference equations for Eq. (40) are

$$h_j^{-1}(E_j^n - E_{j-1}^n) = G_{j-1/2}^n \tag{42a}$$

$$\frac{h_j^{-1}}{Pr}(C_j^n G_j^n - C_{j-1}^n G_{j-1}^n) + (b_3)_{j-1/2}^n G_{j-1/2}^n - 2w_{j-1/2}^{n-1/2} \alpha_n E_{j-1/2} = R_{j-1/2}^{n-1} \tag{42b}$$

Here

$$(b_3)_{j-1/2}^n = (b_2)_{j-1/2}^n + \alpha_n (g_{j-1/2}^n - g_{j-1/2}^{n-1}) \tag{43a}$$

$$(L_3)_{j-1/2}^{n-1} = \frac{h_j^{-1}}{Pr}[C_j^{n-1} G_j^{n-1} - C_{j-1}^{n-1} G_{j-1}^{n-1}] + h_j^{-1}[(b_1)_j^{n-1} - (b_1)_{j-1}^{n-1}] + (b_2)_{j-1/2}^{n-1} G_{j-1/2}^{n-1} \tag{43b}$$

$$R_{j-1/2}^{n-1} = -(L_3)_{j-1/2}^{n-1} - h_j[(b_1)_j^n - (b_1)_{j-1}^n] - \alpha_n [2w_{j-1/2}^{n-1/2} E_{j-1/2}^{n-1} + G_{j-1/2}^{n-1}(g_{j-1/2}^n - g_{j-1/2}^{n-1})] \tag{43c}$$

The boundary conditions for the energy equation become

$$G_0^n = 0 \qquad E_J^n = 1 \tag{44}$$

Noting that the energy equation is linear once the solution of the two momentum equations is obtained; we can write Eq. (42) as

$$(\zeta_1)_j G_j^n + (\zeta_2)_j G_{j-1}^n + (\zeta_3)_j E_j^n + (\zeta_3)_j E_{j-1}^n = R_{j-1/2}^{n-1} \tag{45}$$

where

$$(\zeta_1)_j = \frac{h_j^{-1}}{Pr} C_j^n + \tfrac{1}{2}(b_3)_{j-1/2}^n \tag{46a}$$

$$(\zeta_2)_j = \frac{-h_j^{-1}}{Pr} C_j^n + \tfrac{1}{2}(b_3)_{j-1/2}^n \tag{46b}$$

$$(\zeta_3)_j = -w_{j-1/2}^{n-1/2} \alpha_n \tag{46c}$$

Again the system given by Eqs. (44) and (45) is solved by using the block-elimination method. In this case, we have $2J+2$ equations in as many unknowns and the block tridiagonal system has 2×2 blocks.

Comments on the Solution Algorithm

The present method is developed in such a way that one can use nonuniform net spacings in the streamwise direction and across the boundary layer. In the latter case, the variable grid is a geometric progression having the property that the ratio of lengths of any two adjacent intervals is a constant; that is, $h_j = K h_{j-1}$. The distance to the jth line is given by the following formula:

$$\eta_j = h_1 (K^j - 1)/(K - 1) \qquad (K > 1) \tag{47}$$

There are two parameters: h_1, the length of the first $\Delta\eta$ step, and K, the ratio of two successive steps. The total number of points J can be calculated by the following formula:

$$J = \frac{\ell n [1 + (K-1)(\eta_\infty / h_1)]}{\ell n K} \tag{48}$$

For further details, see Ref. 4.

Often the laminar flow calculations are done for a uniform grid across the boundary layer. However, for flows with suction a variable grid such as the one discussed here would be very useful since, with suction, the velocity profile changes considerably close to the wall. Also, for stability calculations such a grid becomes extremely useful and is needed on account of the critical layer.

Results

To test and demonstrate our method we present a sample calculation for the X-21 wing. The chordwise pressure distribution for $C_L = 0.30$ and $M_\infty = 0.80$ was obtained from p. 79 of Ref. 6. To simulate the suction mass flow rate, we used flight test data from pp. 64-1299 of Ref. 7 with an arbitrary fairing to smooth the data. The test data were for

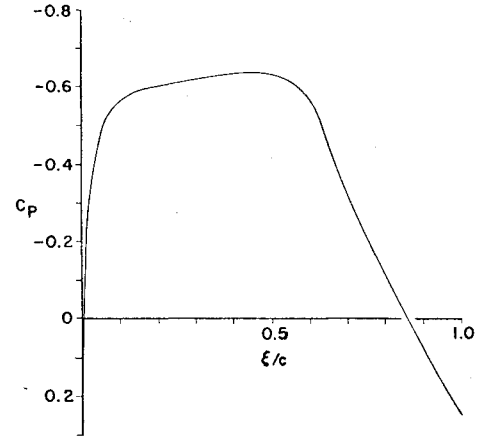

Fig. 3 Upper surface chordwise pressure distribution for the test case: $M_\infty = 0.80$, $C_L = 0.3$.

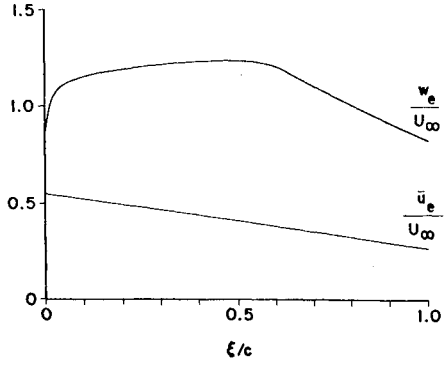

Fig. 4 Calculated inviscid velocity components in polar coordinates.

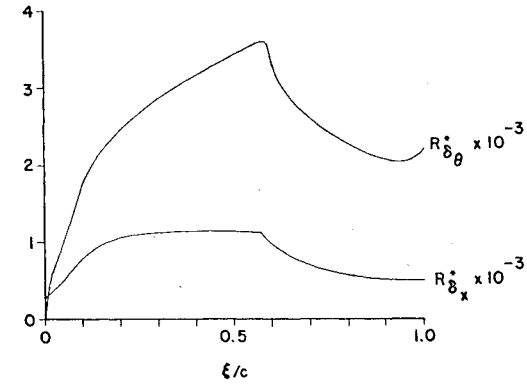

Fig. 6 Calculated displacement thickness Reynolds number distributions with wall suction.

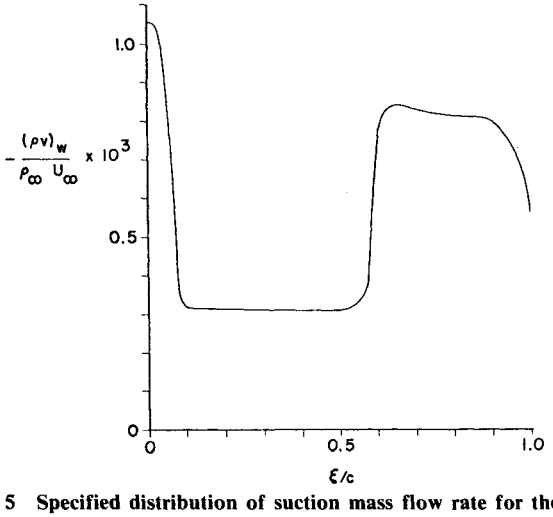

Fig. 5 Specified distribution of suction mass flow rate for the test case.

$M_\infty = 0.80$ at an altitude of 40,000 ft and at an airplane lift coefficient around 0.30. The streamwise airfoil section was represented by the NACA 65A210 airfoil which was the basic section from which the wing was developed. Calculation with the wing geometry yielded the following: leading-edge sweep = 33.2°, trailing edge = 19.1°, and a mean aerodynamic chord length of 14.66 ft. The unit Reynolds number for the flight condition in standard atmosphere is 1.53×10^6/ft which gives a chord Reynolds number of 22.5×10^6.

Figure 3 shows the input pressure distribution used to calculate the radial ($\bar{u}_e$) and the circumferential (w_e) velocity components. Velocity components are shown in Fig. 4. The specified suction distribution, which is typical for a swept wing with laminar flow airfoils, is shown in Fig. 5. Near the leading edge, where the external streamlines are highly curved, the boundary layer exhibits a large crossflow component and as a consequence, becomes susceptible to three-dimensional disturbances. As a rule, considerable suction is required here to keep the flow laminar. This is contrary to the two-dimensional case where the favorable pressure gradient is usually sufficient to keep the flow laminar without employing suction. On the stagnation line itself the crossflow is zero, but two-dimensional disturbances in the form of turbulence contamination from the fuselage boundary layer will increase the suction requirement beyond the theoretical predictions. In the regions of weak favorable pressure gradient, the external streamline curvature is small and the boundary layer reverts to near two-dimensional flow in which two-dimensional disturbances dominate. The small amount of suction required in this region is needed primarily to keep the boundary layer from growing too fast. Note that the strong suction ahead of this region and the favorable pressure gradient have their effects on the mixing of the boundary layer. In the adverse pressure gradient flow the crossflow component grows and the three-dimensional disturbances become the dominant mode. Suction requirement again is increased. Figure 6 shows the calculated displacement thickness Reynolds number distribution plotted against a fraction of chord. It is seen clearly that the allowable Reynolds numbers based on displacement thickness are reduced when the flow encounters adverse pressure gradients on a swept wing. This situation is similar to the two-dimensional case although the mechanism for the initial disturbances may be quite different.

In principle, the tapered wing calculations with conical-flow assumptions are similar to the yawed infinite wing treatment but differ by the inclusion of spanwise divergence or taper effect. As can be inferred from Fig. 4, the calculated spanwise velocity component $\bar{u}_e$ is very close to the value obtained from the local sweep theory. However, there is no single sweep angle for which the yawed infinite wing calculation could match the tapered wing calculation everywhere. It seems that best overall agreement could be obtained with a sweep angle based on the 50% chord point instead of the customary quarter-chord sweep angle.

In conjunction with the trapezoidal planform assumption, the following must be observed with respect to the sweep angles: $\tan\lambda_1 > \tan\lambda_2 > 0$. That is, both the leading and trailing edges must have sweepback. The real limiting factor is, however, the velocity $\bar{u}_e$ which cannot be negative because of the singularity introduced into the transformation when $\bar{u}_e$ goes through zero. For example, in the case of a tapered flat plate with a trailing edge sweep angle λ_2 equal to $-\lambda_1$, the radial velocity $\bar{u}_e$ at zero incidence is equal to $u_\infty \sin\lambda_1$ at the leading edge, it decreases to zero at midchord, and is negative on the rear half of the plate.

Conclusions

We have presented in this paper a method for the calculation of compressible laminar boundary layers on tapered wings with permeable walls. The conical-flow approximations employed restrict application to certain configurations and flight conditions under which the basically three-dimensional flow presents an almost two-dimensional problem. Fortunately, these conditions are precisely those which prevail on a typical laminar flow control wing at design conditions. That is, straight isobars over most of a tapered high-aspect-ratio wing. Calculations at different spanwise stations are made independent of each other by relaxing the strict similarity requirement.

The equations are solved by an efficient two-point finite-difference method. Computing time (CPU) for the test case consisting of 33 streamwise stations and 54 to 93 points across the boundary layer was about 9 sec on the IBM 370/165 computer. The computer program and instructions for its use are described in Ref. 8.

Acknowledgment

This work was supported by NASA Langley Research Center, Hampton, Va., under Contract NAS1-14498.

References

[1] Keller, H. B., "A New Difference Scheme for Parabolic Problems," *Numerical Solutions of Partial Differential Equations*, Vol. II, edited by J. Bramble, Academic Press, New York, 1970.

[2] Cebeci, T. and Bradshaw, P., *Momentum Transfer in Boundary Layers*, Hemisphere and McGraw Hill, 1977.

[3] Keller, H. B. and Cebeci, T., "Accurate Numerical Methods for Boundary Layers. II. Two-Dimensional Turbulent Flows," *AIAA Journal*, Vol. 10, Sept. 1972, pp. 1197-1200.

[4] Cebeci, T. and Smith, A.M.O., *Analysis of Turbulent Boundary Layers*, Academic Press, New York, 1974.

[5] Isaacson, E. and Keller, H. B., *Analysis of Numerical Methods*, Wiley, New York, 1966.

[6] Anon., "The Laminar Flow Control Presentation for the Aeronautical Systems Division," May 3-4, 1962, Northrop Corporation, Norair Division, NB62-105, July 1962.

[7] Anon., "Air Force Review of X-21A Program," Pt. 2, Northrop Corporation, Norair Division, NB64-149, June 1964.

[8] Kaups, K. and Cebeci, T., "Compressible Laminar Boundary Layers with Suction on Swept and Tapered Wings," Douglas Aircraft Corp., Rept. No. MDC J7337, Sept. 1976.